Radiation Protection Dosimetry (2008), pp. 1–7 doi:10.1093/rpd/ncn236

ADVANCED RADIATION MEASUREMENT TECHNIQUES IN DIAGNOSTIC RADIOLOGY AND MOLECULAR IMAGING

Alberto Del Guerra[1,2,*], Nicola Belcari[1,2], Gabriela Llosa Llacer[1], Sara Marcatili[1,2], Sascha Moehrs[1,2] and Daniele Panetta[1,2]
[1]Department of Physics "E. Fermi", University of Pisa, Largo Bruno Pontecorvo, 3, 56127 Pisa, Italy
[2]Istituto Nazionale di Fisica Nucleare, Sezione di Pisa, Pisa, Italy

This paper reports some technological advances recently achieved in the fields of micro-CT and small animal PET instrumentation. It highlights a balance between image-quality improvement and dose reduction. Most of the recent accomplishments in these fields are due to the use of novel imaging sensors such as CMOS-based X-ray detectors and silicon photomultipliers (SiPM). Some of the research projects carried out at the University of Pisa for the development of such advanced radiation imaging technology are also described.

INTRODUCTION

Since the discovery of X rays by Wilhelm Conrad Roentgen in 1895, ionising radiations have been used as a tool for imaging the structure and the function of living subjects. The continuous evolution of medicine has encouraged the development of a wide variety of imaging modalities to better delineate structure and function of living tissue in a dynamic manner. Most of the recent accomplishments in medical imaging are due to the remarkable and continuous advances in instrumentation for radiation detection as well as to the improvements in computer science both in the hardware and software aspects.

The development of new technologies for medical imaging has been driven by two objectives that are often in contrast: image-quality improvement and dose reduction.

In the following sections, some technological advances recently achieved in the fields of computed tomography (CT) and molecular imaging with positron emission tomography (PET) are reported. In addition, some of the research projects carried out at the University of Pisa for the development of advanced radiation imaging technology are illustrated.

ADVANCES IN COMPUTED TOMOGRAHY

The X-ray CT is an indispensable tool for non-invasive 3-D imaging; its use in medical and biomedical applications has been continuously growing since its introduction in the early 1970s by Hounsfield and Cormack. In the last 10 years, this technique has undergone a dramatic evolution. All the technical improvements of CT have led to faster acquisitions, with a capability to reduce patient doses while maintaining diagnostic image quality. The introduction of spiral CT in 1990 by Kalender *et al.*[(1)] and multirow detectors at the beginning of 2000 represent the two major breakthroughs in CT technology. With a 64-slice scanner, it is possible to take a whole-body scan in less than half a minute. This very high scanning speed, together with the possibility of synchronising the acquisition with the ECG signal, opened the way towards the application of CT in cardiology. Depending on the acquisition protocol and on the reconstruction kernel, isotropic spatial resolution of <0.5 mm can be obtained routinely. A thorough review of the major technical improvements in CT is presented in Kalender[(2)].

Nowadays, the direction of research in CT technology in the clinical environment is mainly focused on a further reduction of both patient doses and scanning times[(3)]. Recent improvements in X-ray tube technology, tube current modulation[(4)] and the use of z-flying focal spot[(5,6)] have led to a substantial reduction in patient dose. In order to further reduce the scanning time, manufacturers tend to increase the number of detector rows mounted in the gantry. This trend is limited mainly by the requirement of constancy of image quality among all the reconstructed slices. In fact, the wider the acceptance angle of the detector, the worse will be the image quality of the peripheral slices. This is due in part to the lack of efficient exact reconstruction algorithms for the cone-beam geometry. In 2002, Katsevich proposed an exact inversion formula for the helical cone-beam geometry[(7)], but it has not been yet introduced in clinical practice because of its heavy computational cost. The most used cone-beam reconstruction algorithm, introduced by Feldkamp *et al* in 1984[(8)], is an approximated generalisation of the exact fan-beam reconstruction formula and leads to reconstruction artefacts that could be unacceptable for the image-quality requirements of clinical CT. At present, the maximum number of detector

*Corresponding author: alberto.delguerra@df.unipi.it

rows in commercial scanners has gone to 320, and it has continued to increase, surpassing expectations. Some groups in the world are studying CT systems based on flat-panel detectors[9]. An alternative approach recently used to improve scan speed (especially in cardiac imaging) is the use of dual-source CT[10].

In parallel to the evolution of clinical CT scanners, dedicated tools for morphological studies of small animals have also been developed[11]. High-resolution CT scanners (microCTs) can give outstanding spatial resolutions, ranging from a few hundred to <1 micron. These performances are obtained by using high-resolution flat-panel X-ray detectors, combined with microfocus X-ray sources. Large area detectors are desirable for these applications, in order to take advantage of greater magnification factors (and hence, greater resolution) without compromising the size of the FoV. Even though the dose limits for mice and rats are less restrictive than those of clinical CT, the main limitation in the high-resolution for *in vivo* imaging of small animals is given by dose. In fact, for a given image-noise level, the dose is inversely proportional to the fourth power of the cubic voxel size. The three parameters, dose, resolution and noise are related by the following formula[2]:

$$\frac{\sigma_\mu}{\langle\mu\rangle} \propto \frac{1}{\Delta x^2 \sqrt{D}} \qquad (1)$$

where Δx is the size of the cubic voxel, D the dose, and σ_μ and $<\mu>$ the standard deviation and the mean value of the reconstructed linear attenuation coefficient, respectively. Typical doses for *in vivo* microCT varies from 100 to 500 mGy[11,12].

A CMOS-based microCT scanner prototype

A microCT prototype was built at the University of Pisa, with the main goal of integrating a morphological scanner[13] to the functional YAP-(S)PET II scanner[14]. This prototype has a fixed source-detector system, and the object to be imaged is placed on a rotating support which can also translate in a direction parallel to the axis of rotation. The system magnification can be adjusted manually in order to select the desired trade-off between resolution and FoV size. The X-ray source (Hamamatsu MFX60KVP) is a microfocus source with a fixed tungsten anode and 150 μm of Be inherent filtration. The source has a maximum voltage of 60 kV, a maximum power of 10 W and with a focal spot size of 7 μm (measured with the edge method). The flat-panel X-ray detector (Rad-Icon Rad-Eye4) is composed by a scintillation layer of Ga_2O_2S:Tb (Gadox), directly coupled to a CMOS imaging sensor. The sensor has 2048×1024 pixels of size 48 μm, for a total active area of 98.3×43.2 mm^2. Using a narrow slit of 10 μm aperture, an line spread function (LSF) of width $\sigma_{LSF} = 40$ μm was measured. This value corresponds to an intrinsic resolution of 8.5 lp mm^{-1} at 10% of modulation transfer function (MTF).

At magnification $m = 2$, a high-contrast spatial resolution of 55 μm full width at half maximum (FWHM) in the transaxial plane was obtained, corresponding to a resolution of 14 lp mm^{-1} at 10% of MTF. In order to enhance soft-tissue detectability without increasing the dose to the sample, the projection data can be rebinned: this causes an increase in counting statistic per bin and a loss in spatial resolution. In this case, a noise level of $\sigma_\mu/<\mu> = 2\%$ in a 3-cm thick cylindrical water phantom was measured, with an entrance dose of 700 mGy, measured with a thermo-luminescence dosimeter (TLD) positioned on the surface of a poly-methyl-methacrylate phantom (4 cm diameter), and a spatial resolution of 260 μm FWHM. As stated in Equation (1), the dose can be reduced at the cost of decreasing spatial resolution and/or increasing image noise. Figures 1 and 2 show some images obtained with the CT prototype.

ADVANCES IN PET IMAGING

PET has moved from a distinguished research tool in physiology, cardiology and neurology to become a major tool for clinical investigation in oncology, in cardiac applications and in neurological disorders. In recent years, PET has gained increasing clinical acceptance as an important functional imaging modality, and whole-body PET with ^{18}F-FDG is nowadays a standard technique for the diagnosis and staging of cancer[15]. In recent years, there has been an increasing focus on dedicated PET systems designed for specific applications in new emerging fields such as molecular medicine, gene therapy, breast cancer imaging and animal imaging.

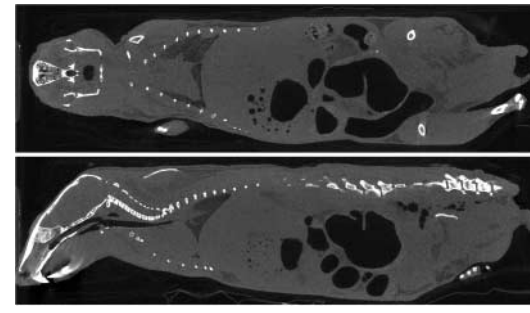

Figure 1. CT images of an *ex vivo* mouse in the coronal view (top) and sagittal view (bottom). The images were reconstructed with a cubic voxel of 82 μm, and the entrance dose was 100 mGy.

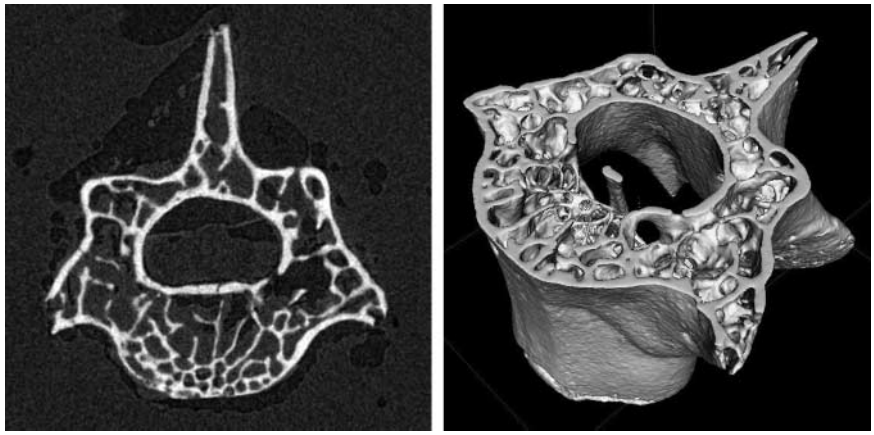

Figure 2. High-resolution reconstruction of a mouse L1 vertebra, with 10 μm cubic voxel size. The trabecular structure of the bone is clearly visible.

Clinical PET instrumentation is nowadays built using well-established technologies, and detector advances in the last 10 years have been mainly focused on the improvement of the spatial resolution that was considered not good enough. The current top-end commercial clinical PET scanners offer a resolution up to 4 mm FWHM[15]. The major concern for the development of the next generation of PET systems is the improvement in sensitivity, still pushing the spatial resolution close to its intrinsic limit. This is particularly true for applications where a small quantity of tracers is used, or when a low tracer specific uptake is observed, such as, for example, in gene research, breast cancer investigation or small animal imaging.

The typical equivalent dose delivered to the patient in a standard PET with ^{18}F-FDG for oncology studies (i.e. the most frequent application) is $\sim$7 mSv. This value is calculated for an injection of 370 MBq of ^{18}F[16]. Owing to the emphasis primarily placed on spatial resolution improvement, the radiation dose has not been reduced significantly in the last 10 years. Further, there is a tendency to utilise PET as a screening technique, i.e. dedicated to potentially healthy people as opposed to the common application as a screening technique oriented to potentially ill people. This requires an appropriate level of justification and consideration of the need to reduce the radiation dose to the patient. In addition, protection of operators is becoming an important factor. As in any other emission imaging technique, dose reduction can be achieved by increasing the sensitivity of the radiation detection instrumentation or applying any technique whose effect is 'equivalent' to an increase in sensitivity, so as to permit the injection of a reduced quantity of radiotracer activity.

Sensitivity improvement by adding more detectors to clinical PET architectures, and thus increasing the geometrical efficiency, is limited not only by additional costs but also by the subsequent increase in computational power required by the greater number of lines-of-response (LORs) that should be considered[17].

Various new technologies have been developed in recent years aimed at increasing sensitivity. In order to maximise the efficiency of the PET system, the PET heads should be positioned close to the object and the thickness of the photon absorber should be at least one attenuation length at 511 keV. In this case, some LORs (especially those having a high geometrical inclination) are subjected to a potentially significant depth-of-interaction (DOI) error. A number of techniques for designing detectors with DOI capability have been proposed, based either on the direct measurement of the DOI within the crystal[18] or by segmenting the crystal into two layers, so that the photodetection system is able to discriminate events occurring in one layer from the other[19,20]. Nowadays, a detector based on a matrix of high Z, fast, scintillating crystals (e.g. LSO:Ce) coupled to a position-sensitive photodetector is a well-established technology and represents the state-of-the-art. To overcome the limitation of present systems, novel materials for γ detection are required in combination with photodetectors able to exploit the crystal's features. For example, a possible improvement of great potential impact would be the reduction of the time resolution of about one order of magnitude. In addition to the obvious reduction of random events, it would become possible to utilise the time-of-flight information for image reconstruction. For example, using new scintillation materials such as $LaBr_3$:Ce, it would be potentially possible to achieve a time resolution of 300–500 ps. Such a figure corresponds to a net reduction of the background variance, which is equivalent to an improvement in sensitivity.

Most of the new technologies that have been and will be transferred to clinical instruments are often preliminary applied and tested on pre-clinical instrumentation, such as small animal scanners. In fact, such instruments should offer a high resolution (close to the PET intrinsic limit) that is usually achieved with finely pixelated scintillating crystal elements. This implies the use, for example, of advanced photodetectors such as position sensitive photomultiplier tubes (PMTs) (PS-PMT).

For example, the small animal scanner YAP-(S)PET[21], originally developed at the Universities of Ferrara and Pisa, is based on 2-mm pitch matrices of YAP:Ce scintillators read out by PS-PMTs. An evolution of this scanner has now been commercialised by I.S.E. srl (http://www.ise-srl.com) under the name YAP-(S)PET II.

The small animal scanner YAP-(S)PET II

Among commercial systems, YAP-(S)PET II[14] is the only scanner that includes PET and SPECT on the same gantry (Figure 3). This is possible because of the four-planar rotating scintillator detectors, made up of a pixelated, medium Z scintillator (YAP:Ce): each matrix is composed of a 4 cm × 4 cm YAP:Ce matrix of 20 × 20 elements, 2 × 2 × 25 mm^3 each, and is coupled to a PS-PMT. SPECT imaging is obtained by simply adding a lead parallel-hole collimator (0.6 mm Ø, 0.15 mm septum) in front of each crystal. Such architecture has the advantage of a reduction of number of detectors, meaning simplicity and affordability in terms of cost and maintenance, but at the same time maintaining the resolution and sensitivity required for pre-clinical applications. The system operates in 3-D data acquisition mode and both filtered back projection and expectation maximisation algorithms can be used for image reconstruction. For both PET and SPECT modalities, the scanner has an axial field of view of 4 cm and the diameter of the transaxial FoV is 4 cm.

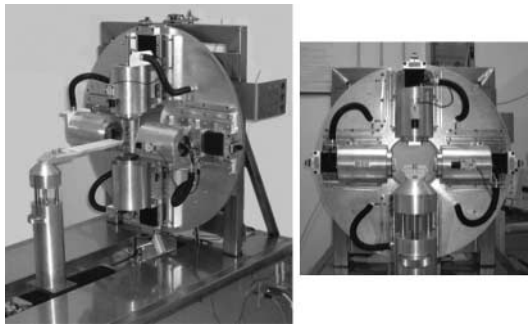

Figure 3. Picture of the small animal scanner YAP-(S)PET II.

In PET mode, it has a maximum volume resolution of ~6.5 mm^3 FWHM at the centre of the FoV and well below 10 mm^3 FWHM over the whole FoV. The maximum sensitivity, measured at the centre of the FoV is ~2.3%. In SPECT mode, the spatial resolution is ~3 mm FWHM, and the sensitivity is 37 cps MBq^{-1}[14]. An example of the application of the YAP-(S)PET in rat brain imaging with PET is shown in Figure 4.

Hybrid systems

PET is a powerful imaging technique that involves tracking biologically significant molecules using positron emitting isotopes to provide exceptionally sensitive assays of a wide range of metabolic processes. A principal drawback of PET is the relatively poor spatial resolution when compared with those of morphological examinations, sometimes hampering unambiguous signal localisation. Further, a quantitative measurement of the sample activity in PET images can only be achieved by means of an accurate attenuation correction obtained from an attenuation coefficient map of the scanned object.

Hence it is advisable to combine PET with techniques that are able to provide morphological information. The combination of PET and CT scanners has already been established producing promising results in the clinical context. CT scans do not only allow anatomical localisation, but also aid in PET image reconstruction and correction for partial volume effects. However, PET and CT cannot be performed simultaneously due to their detector geometry. The possible change in the subject position during the measurement introduces non-rigid movements that are not easily taken into account during image fusion, thus leading to artefacts[22]. In addition, the high-radiation dose necessary for soft-tissue contrast enhancement in CT scans can result in a modified biological response of the subject under screening, altering the model under investigation.

Magnetic resonance imaging (MRI), on the other hand, provides exquisite high-resolution anatomical

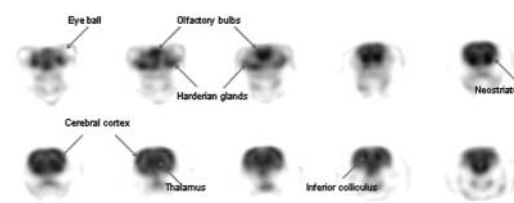

Figure 4. Image of the 18F-FDG metabolism of a rat brain obtained with the YAP-(S)PET scanner (transaxial slices 2-mm thick).

information without exposure to ionising radiation as well as access to volume-specific chemical and physical information (e.g. metabolite concentrations), even though it limited by low-signal strength, leading to a low sensitivity in functional studies[23].

An accurate co-registration of PET and MR images would provide a precise localisation as well as a detailed attenuation map, even though this information is not directly accessible; images need to be segmented into different tissue components, and an attenuation coefficient has to be associated with each element. Moreover, magnetic fields higher than 5 T has been seen to improve the PET spatial resolution by reducing the positron mean-free path[24] representing one of the dominant factors limiting the resolution of state-of-the-art small animal PET scanners.

The complementarity of PET and MRI techniques is evident both in clinical and pre-clinical research applications, and hybrid systems are being eagerly investigated by several research groups[22, 23, 25]. However, the merger is non-trivial, since traditional PET devices are inherently incompatible with MRI physics.

Conventional PET photodetector (PMTs) methods are hindered by the large magnetic field and MRI-dictated geometry constraints. The most common detector for scintillator readout in PET is the PMT whose performance deteriorates in magnetic fields even in the millitesla range. This weakness has prompted widespread investigation of alternative methods of uniting PET and MRI.

One promising solution is to incorporate longer optical fibres (a few metres) to transport the scintillation light outside the high-magnetic field region. On the basis of this model, several prototypes for small animal imaging have been developed[25] and tested in pre-clinical studies, demonstrating the feasibility of the method. However, the use of optical fibres is not without hindrances. The transport of the scintillation light for relatively long distances can cause light loss and fibre cross-talk resulting in degradation of energy and time resolution. In addition, the encouraging results obtained with PMT-based hybrid system cannot be generalised to larger PET configurations where a much greater bulk of material with potential compatibility problems is likely to be required.

Another solution currently under investigation is the use of magnetically insensitive avalanche photodiodes (APD) in place of traditional PMTs. Their compactness allows the assembly of inserters fitting a standard MR bore, even though the amount of shielding needed to prevent pick up from the magnetic gradients could affect MRI quality. However, in spite of overcoming the primary magnetic field problem, such devices are noticeably sensitive to small variations in bias voltage and temperature, and their low gain requires the use of low-noise electronics. These issues become relevant in the presence of rapid MRI gradient coil switching. Furthermore, their low granularity poses limits on the spatial resolution achievable.

A more stable photon detector compatible with high-magnetic field environment remains therefore a necessary next step in the pursuit of dual PET/MRI imaging.

Silicon photomultiplier-based PET for a hybrid system

The use of silicon photomultipliers (SiPMs) appears promising in overcoming the constraints of the current PET/MRI system.

SiPM arrays[26] ($1 \times 1\ mm^2$ pixel size) display properties comparable with those of a traditional PMT with additional advantages[27]. The SiPM is stable and rugged, with excellent single photoelectron resolution, fast recovery time, a high gain (10^6) at low bias voltage ($\sim$35 V) and, most importantly, it is insensitive to magnetic field. The SiPM is a matrix of p–n junction diodes (microcells) biased above the breakdown voltage in order to create a localised Geiger avalanche in each fired microcell[28]. The microcell signals are multiplexed by the common metal electrode contact layer, making it suitable for spectroscopy; this allows the SiPM to provide a large, proportional signal for low-to-moderate photon flux ($N_{photons} \ll N_{cells}$).

The advantage of the SiPM over the more common APD is that it allows a simpler and more reliable use without the need for high bias voltages and low-noise amplifiers.

The goal at the University of Pisa is the assembly of an MR-compatible PET ring tomography to be inserted in a magnet bore for simultaneous PET/MR. The design entails 16 detector heads, each head consisting of a continuous scintillator slab coupled to a finely granulated SiPM matrix (1.5 mm pitch)[29,30].

The feasibility of a combined PET/MRI system based on SiPMs has been proved operating a single SiPM pixel ($1 \times 1\ mm^2$) coupled to an LSO crystal, in an MRI system while running different sequences. Results obtained were fully compatible with those achieved on the bench ($B < 0.5$ mT), and show that the energy resolution is not affected at all by the combined effect of the gradient coils and radiofrequency pulses.

The comparison of single photon spectra acquired in a low-magnetic field with those acquired in a static magnetic field of 1 T plus a pulsed MR gradient (Figure 5) shows that the sensitivity of the SiPM is fully retained in an MRI environment, even at single photon level.

Although it has been confirmed that such a PET scanner would not be adversely affected by the MR system, MRI performances with the scanner placed

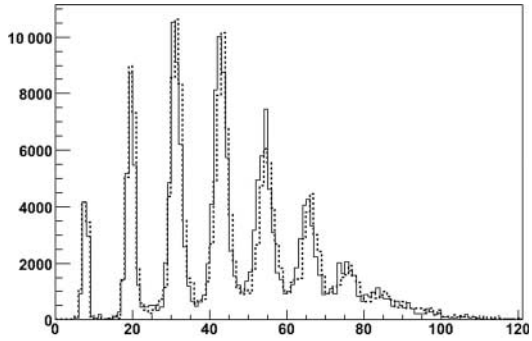

Figure 5. Single photoelectron spectra acquired with the SiPM inside the 1T magnetic field with the gradient on (dotted line) and on the bench (solid line).

in the bore remain to be tested. Despite this, the extremely compact size of this detector and the possibility to attain a good energy resolution without any signal amplification and shaping would limit the amount of material that has to be fit in the bore, reducing potential PET/MRI compatibility problems.

CONCLUSIONS

The technologies for biomedical imaging using ionising radiation are continuously being improved and transferred to the clinical environment. Many of the innovations in this field are also aimed at a reduction of the radiation dose. Technologies are initially tested and applied in small animal imaging instrumentation. The development of PET-MR instrumentation could represent the new frontier for the field of oncology imaging. New technologies for the construction of MR-compatible photodetectors are now available. The characteristics, performance and non-sensitivity to magnetic field of new photodetectors such as SiPM[26,29] justify the interest of various research groups worldwide in the development of large-area SiPM photodetectors for future clinical PET applications.

FUNDING

This work is partially supported by Istituto Nazionale di Fisica Nucleare (INFN-Italy) group V and by a Marie Curie Intra-European Fellowship within the 6th European Community Framework Programme.

REFERENCES

1. Kalender, W. A., Seissler, W., Klotz, E. and Vock, P. *Spiral volumetric CT with single breath hold technique, continuous transport, and continuous scanner rotation.* Radiology **176**(1), 181–183 (1990).
2. Kalender, W. A. *Computed Tomography: Fundamentals, System Technology, Image Quality, Applications*, Second edn. (Publicis MCD Verlag), Erlangen (2005).
3. International Commission on Radiological Protection. *Managing patient dose in multi-detector computed tomography (MDCT)*. ICRP Publication 102, (Pergamon Press), Oxford, Elmsford, N. Y., Ann. ICRP, **37**(1), 1–80 (2007).
4. Kalender, W. A., Wolf, H., Suess, C., Gies, M., Greess, H. and Bautz, W. A. *Dose reduction in CT by online tube current control: principles and validation on phantoms and cadavers.* Eur. Radiol. **9**, 323–328 (1999).
5. Schardt, P., Deuringer, J., Freudenberger, J., Hell, E., Kniipfer, W., Mattern, D. and Schild, M. *New x-ray tube performance in computed tomography by introducing the rotating envelope tube technology.* Med. Phys. **31**(9), 2699–2706 (1999).
6. Kachelriess, M., Knaup, M., Penssel, C. and Kalender, W. A. *Flying focal spot (FFS) in cone-beam CT.* IEEE Trans. Nucl. Sci. **53**(3), 1238–1247 (2006).
7. Katsevich, A. *Theoretically exact FBP-type inversion algorithm for spiral CT SIAM.* J. Appl. Math. **62**, 2012–2026 (2002).
8. Feldkamp, L. A., Davis, L. C. and Kress, J. W. *Practical cone-beam algorithm.* J. Opt. Soc. Am. A **1**, 612–619 (1984).
9. Kalender, W. A. *The use of flat-panel detectors for CT imaging*. Radiologe, **43**(3), 79–87 (2003).
10. Flohr, T. G. *et al. First performance evaluation of a dual-source CT (DSCT) system*. Eur. Radiol. **16**(2), 256–268 (2006).
11. Paulus, M. J., Gleason, S. S., Kennel, S. J., Hunsicker, P. R. and Johnson, D. K. *High resolution X-ray computed tomography: an emerging tool for small animal cancer research.* Neoplasia **2**, 62–70 (2000).
12. Kalender, W., Durkee, B., Langner, O., Stepina, E. and Karolczak, M. *Comparative evaluation: acceptance testing and constancy testing for micro-CT scanners.* Biomed. Tech. **50**(Suppl. 1)(2), 1192–1193 (2005).
13. Panetta, D., Belcari, N., Cicalini, E., Del Guerra, A. and Baldazzi, G. *A high spatial resolution CT scanner prototipe for small animal imaging.* In: Proc. 14th ICMP, Nuremberg, Germany, 14–17 September 2005. Biomed. Techn. **1**, 754 (2005).
14. Del Guerra, A. *et al. Performance evaluation of the fully engineered YAP-(S)PET scanner for small animal imaging*. IEEE Trans. Nucl. Sci. **53**(2), 1078–1083 (2006).
15. Zanzonico, P. *Positron emission tomography: a review of basic principles, scanner design and performance, and current systems.* Semin. Nucl. Med. **34**(2), 87–111 (2000).
16. Brix, G., Lechel, U., Glatting, G., Ziegler, S. I., Muenzing, W., Mueller, S. P. and Beyer, T. *Radiation exposure of patients undergoing whole-body dual-modality ^{18}F-FDG PET/CT examinations.* J. Nucl. Med. **46**(4), 608–613 (2005).
17. Zaidi, H. *Medical image segmentation: Quo Vadis.* Comput. Methods Programs Biomed. **84**(2–3), 63–65 (2006).
18. Moses, W. W. and Derenzo, S. E. *Design studies for a PET detector module using a PIN photodiode to measure depth of interaction*. IEEE Trans. Nucl. Sci. **41**, 1441–1445 (1994).

19. Saoudi, A., Pepin, C. M., Dion, F., Bentourkia, M., Lecomte, R., Andreaco, M., Casey, M., Nutt, R. and Dautet, H. *Investigation of depth-of-interaction by pulse shape discrimination in multicrystal detectors read out by avalanche photodiodes.* IEEE Trans. Nucl. Sci. **46**, 462–467 (1999).
20. Seidel, J., Vaquero, J. J., Siegel, S., Gandler, W. R. and Green, M. V. *Depth identification accuracy of a three layer phoswich PET detector module.* IEEE Trans. Nucl. Sci. **46**, 485–490 (1999).
21. Del Guerra, A., Di Domenico, G., Scandola, M. and Zavattini, G. *High spatial resolution small animal YAP-PET.* Nucl. Instr. Meth. **A409**, 508–510 (1998).
22. Pichler, B. J., Judenhofer, M. S., Catana, C., Walton, J. H., Kneilling, M., Nutt, R. E., Siegel, S. B., Claussen, C. D. and Cherry, S. D. *Performance test of an LSO-APD detector in a 7-T MRI scanner for simultaneous PET/MRI.* J. Nucl. Med. **47**(4), 639–647 (2006).
23. Lucignani, G. *Time-of-flight PET and PET/MRI: recurrent dreams or actual realities?* Eur. J. Nucl. Med. Mol. Imaging **33**(8), 969–971 (2006).
24. Hammer, B. E., Christensen, N. L. and Heil, B. G. *Use of a magnetic field to increase the spatial resolution of positron emission tomography.* Med. Phys. **21**, 1917–1920 (1994).
25. Marsden, P. K., Strul, D., Keevil, S. F., Williams, S. C. R. and Cash, D. *Simultaneous PET and NMR.* Br. J. Radiol. **75**, S53–S59 (2002).
26. Piemonte, C. *Recent progress in the performance of silicon photomultipliers produced at FBK-irst.* IEEE NSS-MIC Conference Records N41-2 (2007).
27. Piemonte, C. *A new silicon photomultiplier structure for blue light detection.* Nucl. Instr. Meth. **A568**, 224–232 (2006).
28. Saveliev, V. and Golovin, V. *Silicon avalanche photodiodes on the base of metal–resistor–semiconductor (MRS) structures.* Nucl. Instr. Meth. **A442**, 223–229 (2000).
29. Llosa, G., Belcari, N., Collazuol, G., Del Guerra, A., Marcatili, S., Moehrs, S. and Piemonte, C. *Silicon photomultipliers and SiPM matrices as photodetectors for scintillator readout in Nuclear medicine.* Conference Record of the IEEE Nuclear Science Symposium and Medical Imaging Conference, Honolulu, USA, October 28–November 3 2007, M14-4, pp. 3220–3223 (2007) ISBN 1-4244-0923-3.
30. Llosa, G., Belcari, N., Collazuol, G., Del Guerra, A., Marcatili, S., Moehrs, S., Piemonte, C. and Stevick, J. W. *Solid state evolution.* Nucl. Eng. Int. **52**(641), 18–20 (2007).